Typhoon-Induced Nonstationary Buffeting Response of Long-Span Bridges

Liang HU* Youlin XU* Wenfeng HUANG** and Hongjun LIU**
*Department of Civil and Structural Engineering,
The Hong Kong Polytechnic University, Kowloon, Hong Kong
**Shenzhen Graduate School,
Harbin Institute of Technology, Shenzhen, China

Abstract
This paper presents a framework for predicting nonstationary buffeting responses of long-span cable-supported bridges under typhoon loading. First, based on the measurement data of typhoon winds, a non-stationary typhoon wind model is proposed, which includes time-varying mean wind speed, mean wind speed profile, and evolutionary power spectral density (EPSD) function. Typhoon loading is correspondingly described as time-varying mean wind force, nonstationary buffeting forces associated with time-dependent aerodynamic coefficients, and self-excited forces characterized by time-dependent aerodynamic derivatives. The analytical method in the time-frequency domain is then developed to compute time-varying mean responses and EPSD-expressed dynamic responses. The proposed framework is finally applied to compute nonstationary buffeting responses of the Stonecutters cable-stayed bridge in Hong Kong under Typhoon Dujuan. The results display the distinct time-varying properties of mean and standard deviation responses of the bridge under Typhoon Dujuan.

Key words: Typhoon wind; nonstationary buffeting response; long-span bridge.

1. Introduction

Many innovative long-span cable-supported bridges emerge in recent years. If these bridges are located in typhoon prone regions, the assurance of functionality and safety of the bridges under typhoons is of the utmost concern. This requires not only accurate models for near-ground typhoon wind, aerodynamic forces, and aeroelastic forces but also meticulous methods and efficient computations for predicting typhoon-induced buffeting responses of long-span bridges.

The buffeting analysis of long-span bridges has been performed for almost fifty years. Davenport (1) introduced a framework for buffeting analysis to quantify effects of unsteadies and spatial variations of wind turbulence. Scanlan (2) introduced flutter derivatives to account for self-excited forces in buffeting analysis. The inability of involving effects of multi-modes and inter-mode coupling was circumvented by fully-coupled 3D buffeting analysis methods (3). Nevertheless, these methods are all based on stationary and Gaussian assumptions.

Typhoon wind exhibits different characteristics from monsoon wind. Although monsoon wind can be probabilistically described by a stationary process, this may not be the case for typhoon wind because of its convective origin. If a bridge site is near typhoon eye walls, changes in wind direction and convective turbulence are considerable. If the bridge site is surrounded by a complex terrain, the profile of typhoon wind and the structure of turbulence become more complicated and evolve with time. Therefore, it is more realistic to model typhoon wind as a non-stationary process and perform nonstationary buffeting analysis of long-span bridges.

This study will therefore first propose, based on the measurement data of typhoon winds, a non-stationary typhoon wind model which includes time-varying mean wind speed, mean wind speed profile, and evolutionary power spectral density (EPSD) function. Typhoon loading is correspondingly described as time-varying mean wind force, nonstationary buffeting forces associated with time-dependent aerodynamic coefficients, and self-excited forces characterized by time-dependent aerodynamic derivatives. The analytical method in the time-frequency domain is then developed to compute time-varying mean responses and EPSD-expressed dynamic responses. The proposed framework is finally applied to compute nonstationary buffeting responses of the Stonecutters cable-stayed bridge subject to Typhoon Dujuan.

2. Typhoon-induced nonstationary winds

2.1 Background

For a long-span bridge, the major wind components which should be considered in buffeting analysis are a longitudinal wind component $U(t)$, perpendicular to the bridge deck in the horizontal plan, and a vertical wind component $W(t)$, perpendicular to the bridge deck in the vertical plan.

The conventional buffeting analysis is based on the assumption that wind speed components are stationary Gaussian stochastic processes and requires four basic elements: (1) mean wind speed; (2) mean wind speed profile; (3) power spectrum; and (4) coherence function. The parameters in the four elements are all time-invariant. However, the boundary layer wind speed components $U(t)$ and $W(t)$ induced by typhoon may not comply with the stationary assumption, and their statistical properties actually evolve with time. Therefore, a nonstationary wind model will be presented in this study by extending the stationary model with instantaneous statistical properties. The term "instantaneous" means that for each time instant the corresponding statistical properties are estimated over a specified time interval whose center is the current time instant.

2.2 Time-varying mean wind speed

In the proposed nonstationary wind model, the longitudinal component $U(t)$ is regarded as the sum of time-varying mean wind speed $\overline{U}(t)$ and zero-mean fluctuating wind speed $u(t)$.

$$U(t)=\overline{U}(t)+u(t) \tag{1}$$

where $\overline{U}(t)$ is defined by short-time averaging over a short time interval T_0:

$$\overline{U}(t)=\frac{1}{T_0}\int_{t-T_0/2}^{t+T_0/2}U(t)\mathrm{d}t \tag{2}$$

T_0 is the basic time-interval and Eq. (2) implies that $\overline{U}(t)$ only contains frequency contents less than $1/T_0$. As a result, the time-varying mean wind speed varies with time very slowly compared with the fluctuating wind speed $u(t)$. The time varying mean wind speed can be further expressed as

$$\overline{U}(t)=\overline{U}_0\cdot\eta_0(t) \tag{3}$$

where $\overline{U}_0$ is the mean of the time-varying mean wind speed $\overline{U}(t)$, which is almost the same as the conventional basic mean wind speed that is time-invariant but depends on the height above the ground z; $\eta_0(t)$ is the time-varying function of mean wind speed, which is assumed to be independent of the height above the ground in this study. In such a way, the conventional mean wind speed profile can be readily incorporated into the nonstationary wind model. The vertical wind component often has a zero mean. Therefore, the vertical component $W(t)$ is regard as only the fluctuating wind speed $w(t)=W(t)$.

2.3 Typhoon mean wind speed profile

During the passage of a typhoon, the mean wind speed profile at a bridge site surrounded by a complex terrain generally does not conform to the traditional logarithmic law or power law. A numerical method for predicting directional typhoon mean wind speed profiles over a complex terrain, $\bar{U}_o(z)$, has been recently proposed by Xu et al. [4]. This method involves the typhoon wind field model, the Monte Carlo simulation, the computational fluid dynamics (CFD) simulation, and the artificial neural networks (ANN).

2.4 Evolutionary spectra

After extracting the time-varying mean wind speed from $U(t)$, the resulted fluctuating wind speed component $u(t)$ may still possess time-varying turbulence characteristics. Therefore, $u(t)$ is regarded as a zero-mean oscillatory process [5] that admits the representation:

$$u(t)=\int_0^{+\infty} A(\omega,t)e^{i\omega t}\,d\xi(\omega) \tag{4}$$

where $i=\sqrt{-1}$; $A(\omega,t)$ is a slowly varying function with time; $\xi(\omega)$ is a zero-mean Gaussian orthogonal increment process having the properties

$$E\left[d\xi(\omega)d\xi(\omega')^*\right]=\begin{cases}0 & \omega\neq\omega' \\ \mu(\omega)d\omega & \omega=\omega'\end{cases} \tag{5}$$

where the superscript "*" denotes complex conjugate; $\mu(\omega)d\omega$ is variance of the increment process. The EPSD of $u(t)$ at time t can then be written as:

$$S_{uu}(\omega,t)=|A(\omega,t)|^2\mu(\omega) \tag{6}$$

In consideration of the nature of typhoon wind, a closed-form formula for $S_{uu}(\omega,t)$ can be proposed by incorporating stationary power spectral density functions with time-varying parameters. In this study, the von Karman spectrum is selected to have the evolutionary von Karman spectrum with time-varying variance, mean wind speed, and integral length scale.

$$\frac{S_{uu}(\omega,t)}{\sigma_u^2(t)}=\frac{1}{2\pi}\frac{\dfrac{4L_u(t)}{\bar{U}(t)}}{\left[1+70.8\left(\dfrac{4\omega L_u(t)}{2\pi\bar{U}(t)}\right)^2\right]^{\frac{5}{6}}} \tag{7}$$

where $L_u(t)$ is the time-varying integral length scale; and $\sigma_u^2(t)$ is the time-varying variance of $u(t)$.

$$\sigma_u^2(t)=\frac{1}{T_U}\int_{t-T_U/2}^{t+T_U/2}u^2(t)\,dt \tag{8}$$

The time interval T_U in Eq. (8) should be less than T_0 in order to involve frequency contents higher than $1/T_0$. The time-varying turbulence intensity can be expressed as:

$$I_u(t)=\sigma_u(t)/\bar{U}(t) \tag{9}$$

Similarly, the vertical wind speed component $w(t)$ can also be defined as an oscillatory process with the evolutionary von Karman spectrum as:

$$\frac{S_{ww}(\omega,t)}{\sigma_w^2(t)}=\frac{1}{2\pi}\frac{\frac{4L_w(t)}{\overline{U}(t)}\left[1+755\left(\frac{L_w(t)}{\overline{U}(t)}\right)^2\right]}{\left[1+283\left(\frac{L_w(t)}{\overline{U}(t)}\right)^2\right]^{\frac{11}{6}}} \tag{10}$$

where $\sigma_w^2(t)$ and $L_w(t)$ are the vertical time-varying variance and integral length scale, respectively.

2.5 Coherence function

According to the Priestley's EPSD theory, the coherence functions of oscillatory processes are time-invariant [(6)]. The exponential coherence function used in the stationary wind model can thus be directly adopted for the nonstationary wind model.

$$\gamma_{pp,ij}(\omega)=\exp\left\{-\frac{\omega}{2\pi}\frac{\left[C_{pz}^2(z_i-z_j)^2+C_{py}^2(y_i-y_j)^2\right]^{\frac{1}{2}}}{\frac{1}{2}\left[\overline{U}(z_i)+\overline{U}(z_j)\right]}\right\} \tag{11}$$

where the symbol p can represent u or w; z_i and y_i denote the vertical and lateral coordinates; C_{pz} and C_{py} are decay coefficients. The coherence between the vertical and longitudinal wind components is disregarded in this study. Based on coherence functions, the cross EPSD can be constructed by:

$$S_{pp,ij}(\omega,t)=S_{pp,ii}(\omega,t)S_{pp,jj}(\omega,t)\gamma_{pp,ij}(\omega) \tag{12}$$

3. Typhoon induced nonstationary forces and moment

3.1 Time-varying mean wind forces

For a bridge deck with width B and unit length, the mean wind forces acting on its center due to the nonstationary wind speeds described above can be expressed as

$$L_m(t)=\frac{1}{2}\rho\overline{U}(t)^2C_L(\overline{\alpha}(t))B \tag{13}$$

$$D_m(t)=\frac{1}{2}\rho\overline{U}(t)^2C_D(\overline{\alpha}(t))B \tag{14}$$

$$M_m(t)=\frac{1}{2}\rho\overline{U}(t)^2C_M(\overline{\alpha}(t))B^2 \tag{15}$$

where L_m, D_m and M_m denote the lift force, drag force, and pitching moment, in which the subscript "m" denotes mean value; C_L, C_D and C_M denote aerodynamic lift force, drag force and pitching moment coefficients. These coefficients are related to the instantaneous mean wind attack angle $\overline{\alpha}$.

$$\overline{\alpha}(t)=\overline{\alpha}_0(t)+\overline{\alpha}_S(t) \tag{16}$$

where $\overline{\alpha}_0$ is the attack angle of time-varying mean wind; and $\overline{\alpha}_S$ is the torsional response of the bridge deck due to the time-varying mean wind forces and moment. As a result, $\overline{\alpha}$ is time-varying, and the force coefficients, which depend on $\overline{\alpha}$, are also time-dependent. The mean wind forces and moment evolve with time and should be determined by iteration. Nevertheless, the mean wind forces and moment vary with time very slowly, for the time-varying mean wind speed contains frequency contents less than $1/T_0$.

3.2 Nonstationary self-excited forces

Under typhoon-induced nonstationary wind, the self-excited forces and moment acting on the bridge deck unit can be expressed as

$$L_{se}(t)=\rho B^2\omega\begin{bmatrix} H_1^*(\bar{\alpha}(t),\bar{U}_R(t))\dot{h}(t)+BH_2^*(\bar{\alpha}(t),\bar{U}_R(t))\dot{\alpha}(t)+\omega BH_3^*(\bar{\alpha}(t),\bar{U}_R(t))\alpha(t)+ \\ +\omega H_4^*(\bar{\alpha}(t),\bar{U}_R(t))h(t)+H_5^*(\bar{\alpha}(t),\bar{U}_R(t))\dot{p}(t)+\omega H_6^*(\bar{\alpha}(t),\bar{U}_R(t))p(t) \end{bmatrix} \tag{17}$$

$$D_{se}(t)=\rho B^2\omega\begin{bmatrix} P_1^*(\bar{\alpha}(t),\bar{U}_R(t))\dot{p}_k(t)+BP_2^*(\bar{\alpha}(t),\bar{U}_R(t))\dot{\alpha}(t)+\omega BP_3^*(\bar{\alpha}(t),\bar{U}_R(t))\alpha(t)+ \\ +\omega P_4^*(\bar{\alpha}(t),\bar{U}_R(t))p_k(t)+P_5^*(\bar{\alpha}(t),\bar{U}_R(t))\dot{h}(t)+\omega P_6^*(\bar{\alpha}(t),\bar{U}_R(t))h(t) \end{bmatrix} \tag{18}$$

$$M_{se}(t)=\rho B^3\omega\begin{bmatrix} A_1^*(\bar{\alpha}(t),\bar{U}_R(t))\dot{h}(t)+BA_2^*(\bar{\alpha}(t),\bar{U}_R(t))\dot{\alpha}(t)+\omega BA_3^*(\bar{\alpha}(t),\bar{U}_R(t))\alpha(t)+ \\ +\omega A_4^*(\bar{\alpha}(t),\bar{U}_R(t))h(t)+A_5^*(\bar{\alpha}(t),\bar{U}_R(t))\dot{p}(t)+\omega A_6^*(\bar{\alpha}(t),\bar{U}_R(t))p(t) \end{bmatrix} \tag{19}$$

where L_{se}, D_{se} and M_{se} denote the lift force, drag force, and pitching moment in which the subscript "*se*" denotes self-excited forces; P_i^*, H_i^*, and A_i^* (i=1,..., 6) are the flutter derivatives which are the functions of instantaneous mean wind attack angle and the reduced mean wind speed $\bar{U}_R(t)=2\pi\bar{U}(t)/\omega B$; $h_k(t)$, $p_k(t)$ and $\alpha_k(t)$ are the vertical and lateral dynamic displacement responses and the dynamic torsional response of the bridge deck; and each over-dot denotes differentiation with respect to time. It is noted that the flutter derivatives are functions of time due to indirect effects of the time-varying mean wind speed but they vary with time very slowly.

3.3 Nonstationary buffeting forces

The typhoon-induced nonstationary buffeting forces on the bridge deck can be expressed as:

$$L_b(t)=\frac{1}{2}\rho\bar{U}(t)B\left\{2C_L(\bar{\alpha}(t))u(t)+\left[C_L'(\bar{\alpha}(t))+C_D(\bar{\alpha}(t))\right]w(t)\right\} \tag{20}$$

$$D_b(t)=\frac{1}{2}\rho\bar{U}(t)B\left[2C_D(\bar{\alpha}(t))u(t)+C_D'(\bar{\alpha}(t))w(t)\right] \tag{21}$$

$$M_b(t)=\frac{1}{2}\rho\bar{U}(t)B^2\left[2C_M(\bar{\alpha}(t))u(t)+C_M'(\bar{\alpha}(t))w(t)\right] \tag{22}$$

where the subscript "*b*" denotes buffeting forces; the superscript " $\circ'$ " means the differentiation with respect to the attack angle. Eqs. (20)-(22) are based on the quasi-steady assumption and the unit aerodynamic admittance. Apart from the time-varying mean wind speed, the aerodynamic coefficients and their derivatives are also time-dependent due to the time-dependent attack angle. Furthermore, wind speed components $u(t)$ and $w(t)$ are non-stationary and they have time-varying statistical properties as discussed in Section 2.4.

4. Typhoon-induced nonstationary buffeting responses

4.1 Governing equations of motion

The governing equations of motion for buffeting response analysis of the bridge under typhoon-induced nonstationary winds can be expressed as:

$$\mathbf{M}\ddot{\mathbf{X}}(t)+\mathbf{C}\dot{\mathbf{X}}(t)+\mathbf{K}\mathbf{X}(t)=\mathbf{F}_m(t)+\mathbf{F}_{se}(t)+\mathbf{F}_b(t) \tag{23}$$

where **M**, **C** and **K** are the $N\times N$ mass, damping and stiffness matrices, respectively, of the finite element model of the entire bridge; N is the total number of degree of freedoms; and $\mathbf{X}(t)$ is the N dimensional buffeting response vector of the entire bridge in the global coordinate system. The buffeting response vector is a nonstationary vector process which can be written as

$$\mathbf{X}(t)=\bar{\mathbf{X}}(t)+\mathbf{x}(t) \tag{24}$$

where $\bar{\mathbf{X}}(t)$ and $\mathbf{x}(t)$ denote the time-varying mean wind response and the fluctuating wind response, respectively; $\dot{\mathbf{X}}(t)$ and $\ddot{\mathbf{X}}(t)$ are the nonstationary velocity and acceleration vectors; $\mathbf{F}_m$, $\mathbf{F}_{se}$ and $\mathbf{F}_b$ are the loading vectors of mean wind forces, self-excited forces and buffeting forces.

Suppose that the entire bridge is divided into M units for considering wind loading.

The wind loading vectors can then be expressed as:

$$\mathbf{F}_m(t) = \mathbf{T}_s(t)\mathbf{C}_{bu}(t)\bar{\mathbf{U}}(t) \tag{25}$$

$$\mathbf{F}_{se}(t) = \mathbf{A}_s(t)\mathbf{x}(t) + \mathbf{A}_d(t)\dot{\mathbf{x}}(t) \tag{26}$$

$$\mathbf{F}_b(t) = \mathbf{T}_s(t)\mathbf{C}_b(t)\mathbf{\Theta}(t) \tag{27}$$

where $\bar{\mathbf{U}}(t) = \left[\bar{U}_1(t)\cdots\bar{U}_M(t)\right]$ and $\mathbf{\Theta}(t) = \left[\mathbf{u}(t)^{\mathrm{T}}\ \mathbf{w}(t)^{\mathrm{T}}\right]^{\mathrm{T}}$ are the vectors of time-varying mean wind speeds and nonstationary fluctuating wind speeds; $\mathbf{u}(t) = \left[u_1(t)\cdots u_M(t)\right]^{\mathrm{T}}$ and $\mathbf{w}(t) = \left[w_1(t)\cdots w_M(t)\right]^{\mathrm{T}}$; $\mathbf{C}_b(t) = \left[\mathbf{C}_{bu}(t)\ \mathbf{C}_{bw}(t)\right]$ is the time-dependent aerodynamic force coefficients matrix; $\mathbf{C}_{bu}(t) = \mathrm{diag}\left[\mathbf{C}_{bu}^1(t)\cdots\mathbf{C}_{bu}^M(t)\right]$; $\mathbf{C}_{bw}(t) = \mathrm{diag}\left[\mathbf{C}_{bw}^1(t)\cdots\mathbf{C}_{bw}^M(t)\right]$; and

$$\mathbf{C}_{bu}^k(t) = \frac{1}{2}\rho\bar{U}_k(t)Bl_k\left[2C_{L,k}(t)\quad 2C_{D,k}(t)\quad 2BC_{M,k}(t)\right]^{\mathrm{T}} \tag{28}$$

$$\mathbf{C}_{bw}^k(t) = \frac{1}{2}\rho\bar{U}_k(t)Bl_k\left[C'_{L,k}(t) + C_{D,k}(t)\quad C'_{D,k}(t)\quad BC'_{M,k}(t)\right]^{\mathrm{T}} \tag{29}$$

are the aerodynamic force coefficient matrices related to longitudinal and vertical turbulence components; $\mathbf{A}_s(t) = \mathbf{T}_s(t)\left\{\mathrm{diag}\left[\mathbf{A}_s^1(t)\cdots\mathbf{A}_s^M(t)\right]\right\}\mathbf{T}_s(t)^{\mathrm{T}}$ and $\mathbf{A}_d(t) = \mathbf{T}_s(t)\left\{\mathrm{diag}\left[\mathbf{A}_d^1(t)\cdots\mathbf{A}_d^M(t)\right]\right\}\mathbf{T}_s(t)^{\mathrm{T}}$ are the time-dependent aeroelastic stiffness and damping matrices, in which

$$\mathbf{A}_s^k = \rho B^2\omega^2 l_k\begin{bmatrix} H_{4,k}^*(t) & H_{6,k}^*(t) & BH_{3,k}^*(t) \\ P_{6,k}^*(t) & P_{4,k}^*(t) & BP_{3,k}^*(t) \\ BA_{4,k}^*(t) & BA_{6,k}^*(t) & B^2A_{3,k}^*(t)\end{bmatrix},\quad \mathbf{A}_d^k = \rho B^2\omega l_k\begin{bmatrix} H_{1,k}^*(t) & H_{5,k}^*(t) & BH_{2,k}^*(t) \\ P_{5,k}^*(t) & P_{1,k}^*(t) & BP_{2,k}^*(t) \\ BA_{1,k}^*(t) & BA_{5,k}^*(t) & B^2A_{2,k}^*(t)\end{bmatrix} \tag{30}$$

$\mathbf{T}_s(t)$ is a $N \times M$ dimensional coordinate transformation matrix, which is also time-dependent since it depends on the instantaneous mean wind attack angles.

4.2 Time-varying mean wind response

As mentioned in Section 3.1, the mean wind force vector $\mathbf{F}_m(t)$ evolves with time very slowly. Therefore, although the mean wind response shall be predicted for each time instant, the prediction can be performed by static analysis without considering dynamic effects. The basic equation for static analysis can be derived from Eq. (23) at the rth time instant.

$$\mathbf{K}\bar{\mathbf{X}}(t_r) = \mathbf{F}_m\left(\bar{\mathbf{U}}(t_r), \bar{\boldsymbol{\alpha}}(t_r)\right) \tag{31}$$

Nevertheless, the above equation is a nonlinear equation because the mean wind attack angle vector $\bar{\boldsymbol{\alpha}}(t_r)$ depends on the mean wind response vector $\bar{\mathbf{X}}(t_r)$. An iterative procedure shall be introduced to find both $\bar{\boldsymbol{\alpha}}(t_r)$ and $\bar{\mathbf{X}}(t_r)$. The resulted time-varying mean wind attack angle $\bar{\boldsymbol{\alpha}}(t)$ within the concerned time period will be used for the dynamic response analysis.

4.3 Modal equations for nonstationary buffeting responses

By using the modal superposition method and eliminating the time-varying mean wind force and response, Eq. (23) can be transformed into

$$\ddot{\mathbf{q}}(t) + \tilde{\mathbf{C}}(t)\dot{\mathbf{q}}(t) + \tilde{\mathbf{K}}(t)\mathbf{q}(t) = \mathbf{Q}_b(t) \tag{32}$$

where $\tilde{\mathbf{C}}(t) = \mathbf{\Phi}^{\mathrm{T}}\mathbf{C}\mathbf{\Phi} - \mathbf{\Phi}^{\mathrm{T}}\mathbf{A}_d(t)\mathbf{\Phi}$ and $\tilde{\mathbf{K}}(t) = \mathbf{\Lambda} - \mathbf{\Phi}^{\mathrm{T}}\mathbf{A}_s(t)\mathbf{\Phi}$ are the generalized modal damping and stiffness matrices, and they are time-dependent; $\mathbf{Q}_b(t) = \mathbf{\Phi}^{\mathrm{T}}\mathbf{F}_b(t)$ is the generalized buffeting force vector; and $\mathbf{\Phi}$ is the modal matrix reserving only the first N_S order of structural modes and it is normalized as

$$\mathbf{\Phi}^{\mathrm{T}}\mathbf{M}\mathbf{\Phi} = \mathbf{I}_{N_S\times N_S},\quad \mathbf{\Phi}^{\mathrm{T}}\mathbf{K}\mathbf{\Phi} = \mathbf{\Lambda} = \mathrm{diag}(\omega_j^2),\quad j = 1\ldots N_S \tag{33}$$

in which ω_j is the jth natural frequency of the bridge; $\mathbf{q}(t)$ denotes the generalized modal coordinate vector such that

$$\mathbf{x}(t) = \mathbf{\Phi}\mathbf{q}(t) \tag{34}$$

It is noted that $\mathbf{Q}_b(t)$ in Eq. (32) is a N_S dimensional nonstationary Gaussian vector process with zero mean, characterized by the EPSD matrix rather than the PSD matrix:

$$\mathbf{S}_{\mathbf{Q}_b\mathbf{Q}_b}(\omega,t) = \mathbf{\Phi}^{\mathrm{T}}\mathbf{S}_{\mathbf{F}_b\mathbf{F}_b}(\omega,t)\mathbf{\Phi} = \mathbf{\Phi}^{\mathrm{T}}\mathbf{T}_s(t)\mathbf{C}_b(t)\mathbf{S}_{\mathbf{VV}}(\omega,t)\mathbf{C}_b(t)^{\mathrm{T}}\mathbf{T}_s(t)^{\mathrm{T}}\mathbf{\Phi} \tag{35}$$

4.4 Pseudo excitation method for solving modal equations

The pseudo excitation method (PEM) is a highly efficient and accurate method for random vibration analysis [7] and it has been used for stationary buffeting analysis of the bridge. The PEM is extended in this study to solve Eq. (32) in the time-frequency domain. First, the pseudo excitation vector is defined as

$$\tilde{\mathbf{Q}}_{b,j}(\omega,t)=\mathbf{A}_{\mathbf{Q}_b,j}(t,\omega)\mathrm{e}^{\mathrm{i}\omega t} \tag{36}$$

where the matrix $\mathbf{A}_{\mathbf{Q}_b}(t,\omega)$ can be obtained by the Cholesky decomposition of the EPSD matrix $\mathbf{S}_{\mathbf{Q}_b\mathbf{Q}_b}(\omega,t)$, which satisfies

$$\mathbf{S}_{\mathbf{Q}_b\mathbf{Q}_b}(\omega,t)=\mathbf{A}_{\mathbf{Q}_b}(t,\omega)\mathbf{A}_{\mathbf{Q}_b}(t,\omega)^{\mathrm{T}} \tag{37}$$

By replacing the loading term $\mathbf{Q}_b(t)$ in Eq. (32) with the pseudo excitation $\tilde{\mathbf{Q}}_{b,j}(\omega,t)$, the response $\mathbf{y}_j(\omega,t)$ can then be obtained

$$\mathbf{y}_j(\omega,t)=\int_0^t\mathbf{h}(t-\tau,\tau)\mathbf{A}_{\mathbf{Q}_b,j}(\tau,\omega)\mathrm{e}^{\mathrm{i}\omega\tau}\,\mathrm{d}\tau \tag{38}$$

where $\mathbf{h}(t-\tau,\tau)$ is the time-dependent impulse response matrix of the dynamic system expressed by Eq.(32). $\mathbf{y}_j(\omega,t)$ can be found numerically by the Newmark integration method. Consequently, the EPSD matrix of buffeting responses $\mathbf{x}(t)$ can be obtained as

$$\mathbf{S}_{\mathbf{xx}}(\omega,t)=\sum_{j=1}^{N_S}\left[\mathbf{\Phi}\mathbf{y}_j(\omega,t)\right]^*\left[\mathbf{\Phi}\mathbf{y}_j(\omega,t)\right]^{\mathrm{T}} \tag{39}$$

Once the EPSD matrix is obtained, other statistics such as time-varying standard deviation of the nonstationary buffeting responses can be finally computed readily. A study aiming at estimating peaks of the nonstationary buffeting responses is also in progress.

5. Application to Stonecutters bridge

5.1 Brief description of the bridge

The Stonecutters Bridge in Hong Kong is the second longest cable-stayed bridge in the world with a main span of 1018m. This bridge is not only located in one of the most active typhoon regions but also surrounded by a complex terrain, which makes wind field possess distinct nonstationary characteristics. A 3-D finite element model of the Stonecutters Bridge has been established by using the ANSYS software package and updated based on measured modal properties. By using the updated model, the first 20 natural frequencies and modal shapes are computed and used for the nonstationary buffeting analysis. A modal damping ratio 2% is adopted for each mode of vibration. Wind forces are supposed to act on the bridge deck, bridge tower, and bridge piers at the nodes shown in Figure 1. The aerodynamic coefficients and flutter derivatives of the bridge deck were provided by the Hong Kong Highways Department and obtained from wind tunnel sectional model tests.

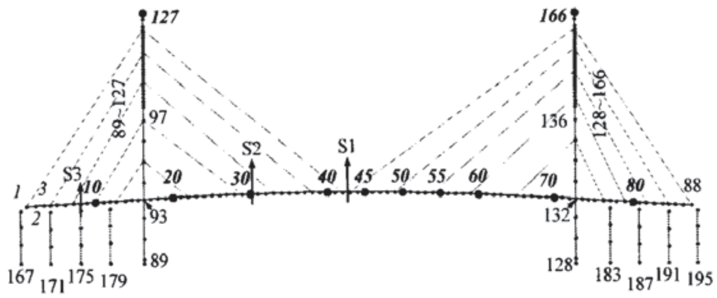

Figure 1 Stonecutters bridge with wind force node number

5.2 Typhoon-induced nonstationary wind

Typhoon Dujuan affected the Stonecutters bridge site on 29th August 2003. The field measurement system near the bridge site recorded wind speed time-histories at a 30m height above the ground [8]. The measured longitudinal wind speed time history $U(t)$ of one-hour duration is shown in Figure 2 (a). The time-varying mean wind speed $\overline{U}(t)$ is estimated by using the short-time averaging over $T_0 = 600\text{s}$, and the result is shown in Figure 2 (a). The fluctuating wind speed time history $u(t) = U(t) - \overline{U}(t)$ is then computed and displayed in Figure 2 (b). The time-varying variance is also estimated by using the short-time averaging with a time window $T_U = 128\text{s}$ and the resulted $\sigma_u^2(t)$ is shown in Figure 2 (b). The time-varying turbulence intensity $I_u(t)$ is obtained by using Eq.(9). The EPSD function $S_{uu}(\omega,t)$ of the fluctuating wind speed $u(t)$ can be obtained by using a method proposed by Priestley [5].

$$U(\omega_p,t_r) = \left[g(t_r)\right] * \left[u(t_r)\exp(-\mathrm{i}\omega_p t_r)\right] \tag{40}$$

$$S_{uu}(\omega_p,t_r) = \left[W(t_r)\right] * \left[\left|U(\omega_p,t_r)\right|^2\right] \Box 2(\Delta t)^3 \tag{41}$$

where the symbol " * " denotes the discrete convolution; $t_r = (r-1)\Delta t$ and $\omega_p = (p-1)\Delta\omega$ are the discrete time and frequency. In this application, $\Delta t = 0.25\text{s}$ and $\Delta\omega = 0.0491\text{rad/s}$. $g(t)$ and $W(t)$ both are the window functions chosen as

$$g(u) = \begin{cases} 1/2\sqrt{h\pi} & (|u| \le h) \\ 0 & (|u| > h) \end{cases} \tag{42}$$

$$W_{T'}(t) = \begin{cases} 1/T' & (-T'/2 \le t \le T'/2) \\ 0 & \text{otherwise} \end{cases} \tag{43}$$

where the window lengths are selected as h=16s and T'=128s. Because the nonstationary analysis is time-consuming, only the wind speed time history of 512s duration, as indicated in Figure 2 and shown in Figure 3, is considered for buffeting response analysis.

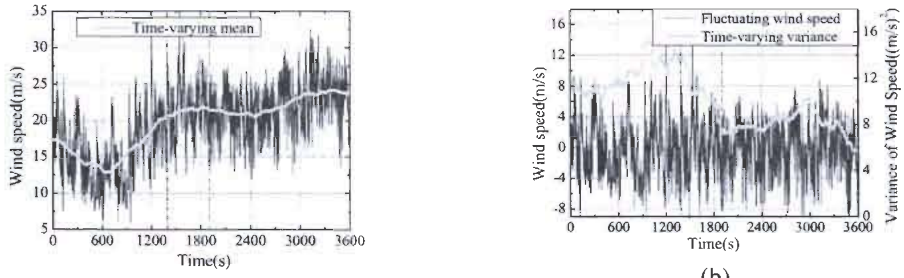

(a) (b)

Figure 2 Longitudinal wind speed time history (a) original time history with time-varying mean wind speed; (b) fluctuating wind speed with time-varying variance.

Within the specified time duration, $\overline{U}(t)$ and $I_u(t)$ can be fitted using the least squares method by the following empirical formulas:

$$\overline{U}(t) = 18.43 + 0.0032t + 0.0087 + 0.081\sin(0.021t + 1.73) \tag{44}$$

$$I_u(t) = \begin{cases} 0.14 + 9.15\times10^{-5}t + 0.0042\sin(0.082t + 0.55) & 0 \le t < 225\text{s} \\ 0.18 - 5.85\times10^{-5}t - 0.022\exp\left[-\left(\dfrac{t-258.92}{31.34}\right)^2\right] & 225 \le t < 270\text{s} \\ 1.56\times10^{-6}t^2 - 0.0012t + 0.34 & 270 \le t < 370\text{s} \\ 0.29 - 5.85\times10^{-5}t - 0.15\exp\left[-\left(\dfrac{t-410.67}{154.72}\right)^2\right] & 370 \le t < 512\text{s} \end{cases} \tag{45}$$

They are shown in Figure 4 and Figure 5 in comparison with the measured ones. Within the specified time duration, the evolutionary von Karman spectrum can be found by using $\overline{U}(t)$, $I_u(t)$, and the EPSD function $S_{uu}(\omega,t)$. Then, the time-varying integral scale $L_u(t)$ can be found and fitted by the following empirical formula:

$$L_u(t) = \begin{cases} 54.36 - 0.036t + 66.19\exp\left[-\left(\dfrac{t-157}{139.89}\right)^2\right] & 0 \le t < 225\text{s} \\ -0.15t + 131 & 225 \le t < 270\text{s} \\ 87.93 - 0.036t + 25.64\exp\left[-\left(\dfrac{t-294.57}{31.99}\right)^2\right] & 270 \le t < 370\text{s} \\ 98.30 - 0.036t - 10.82\sin(0.027t - 2.42) & 370 \le t < 512\text{s} \end{cases} \tag{46}$$

The time-varying integral scale is shown in Figure 6. The measured and modeled EPSD of longitudinal wind speed are shown in Figure 8(a) and Figure 8(b) respectively.

The mean wind profile and the coherence function cannot be obtained from the measurement data. The mean wind speed profile shown in Figure 7, which is obtained by a CFD simulation with the topographic model around the bridge site and typhoon Dujuan wind data [4], is used. For the coherence function, the decay coefficients C_{pz} and C_{py} are taken as 8.3 and 6.4 for $p=u$ and 3.8 and 4.8 for $p=w$.

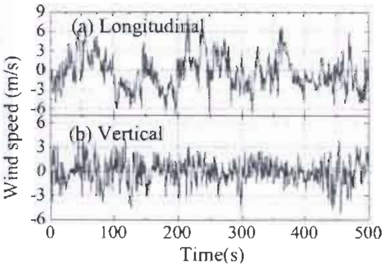

Figure 3 Specified 10-min typhoon wind speed time histories.

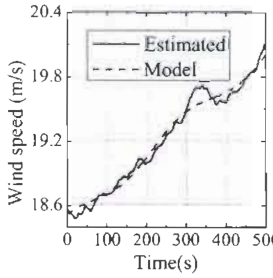

Figure 4 Time-varying mean wind speed

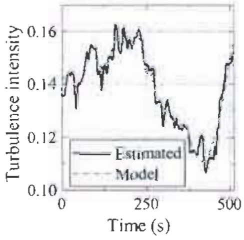

Figure 5 Time-varying longitudinal turbulence intensity

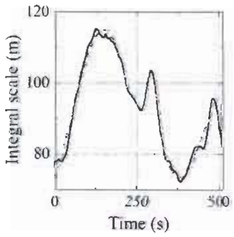

Figure 6 Time-varying longitudinal integral scale

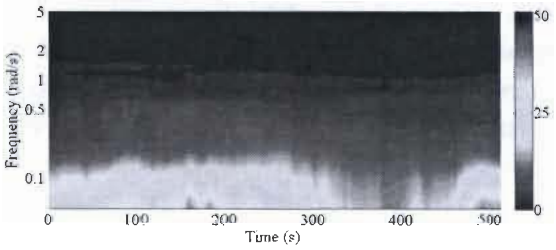

(a) Measured

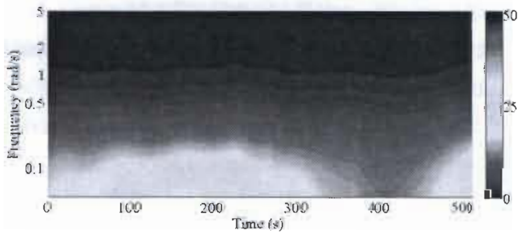

(b) Fitted

Figure 8 Measured and fitted EPSD of longitudinal fluctuating wind speed.

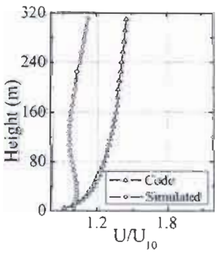

Figure 7 Typhoon mean wind speed profile

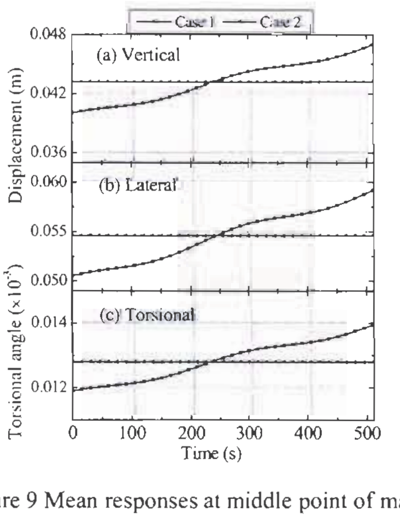

Figure 9 Mean responses at middle point of main span.

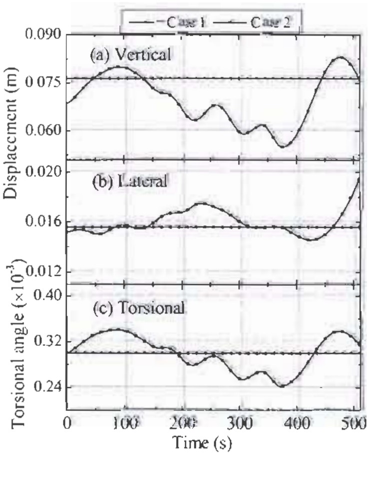

Figure 10 Standard deviations of responses at middle point of main span.

5.3 Typhoon-induced buffeting responses

To assess the effects of nonstationary typhoon wind on buffeting responses of the bridge, both the nonstationary buffeting analysis using the proposed method (Case 1) and the conventional stationary buffeting analysis by regarding the mean wind is constant and the PSD function is time-invariant (Case 2) on purpose are performed and compared with each other. It should be pointed out that the conventional stationary buffeting analysis cannot be performed in principle because typhoon wind is nonstationary.

The computed mean and standard deviation of responses are shown in Figure 9 and Figure 10, respectively. In each figure, the subplots (a)-(c) are associated with the vertical, lateral, and torsional displacements of Location S1 of the bridge as shown in Figure 1. It can be observed that both mean and standard deviation responses computed by the nonstationary model display distinct time-varying properties, and these responses alter around the corresponding time-invariant responses obtained from the stationary model. Furthermore, at the time interval from 450s to 512s, the time-varying mean and standard deviation responses of the bridge predicted by the nonstationary model are larger than those obtained from the stationary model.

6. Concluding Remarks

A framework for predicting nonstationary buffeting responses of a long-span bridge surrounded by a complex terrain and under typhoon-induced wind loading has been presented and applied to the Stonecutters cable-stayed bridge in Hong Kong under Typhoon Dujuan. The numerical results demonstrate the distinct time-varying properties of mean and standard deviation responses of the bridge subject to nonstationary typhoon winds.

References

(1) Davenport, A. G., Buffeting of a suspension bridge by storm winds, J. Struct. Eng.-ASCE, Volume 8(3), 1962, pp. 233-269.

(2) Scanlan, R. H., Action of flexible bridges under wind, .2. Buffeting theory, J. Sound Vibr., Volume 60(2), 1978, pp. 201-211.

(3) Chen, X., and Kareem, A., Advances in modeling of aerodynamic forces on bridge decks, J. Eng. Mech.-ASCE, Volume 128(11), 2002, pp. 1193-1205.

(4) Xu, Y.L., Huang, W.F. and Liu, H.J., Prediction of typhoon wind speed and profile over complex terrain. Submitted to J. Wind Eng. Ind. Aerodyn.

(5) Priestley, M. B., Evolutionary spectra and non-stationary processes, J. R. Stat. Soc. Ser. B-Stat. Method, Volume 27(2), 1965, pp. 204-237.

(6) Mélard, G., and Schutter, A. H.-D, Contributions to evolutionary spectral theory, J. Time Ser. Anal., Volume 10(1), 1989, pp. 41-63.

(7) Lin, J. H. and Zhang, Y. H., Pseudo Excitation Method in Random Vibration, Science Press, Beijing, China, 2004. (in Chinese)

(8) Chen, J., Hui, M. C. H., and Xu, Y. L., A comparative study of stationary and non-stationary wind models using field measurements, Bound.-Layer Meteor., Volume 122(1), 2007, pp. 105-121.

Acknowledgements

The work described in this paper was financially supported by the Hong Kong Polytechnic University through its Niche Area Programs (PolyU 1-BB20 and 1-BB68), by the Natural Science Foundation of China through its key program (NSFC 50830203). The support from the Highways Department of Hong Kong to allow the authors to access the field measurement data for academic purpose only is particularly appreciated. Any opinions and concluding remarks presented in this paper are entirely those of the authors.